



# OPEN Assessment of target-enrichment library preparation and next-generation sequencing of paraffin-embedded gastric biopsies for *H. pylori* diagnosis and evaluation of virulome and resistome

Léo Gillet<sup>1</sup>, Claudie Perreau<sup>1</sup>, Lucie Bruhl<sup>1</sup>, Quentin Jehanne<sup>1</sup>, Marion Marty<sup>2</sup>, Maxence Rauturier<sup>2</sup>, Geneviève Belleannée<sup>2</sup>, Marie Parrens<sup>2</sup>, Pierre Dubus<sup>3,4,5</sup> & Philippe Lehours<sup>1,4,5,6</sup>✉

The diagnosis of *Helicobacter pylori* infection from gastric biopsies requires polymerase chain reaction or culture. However, culture is often unsuccessful due to the bacterial fragility and complex growth requirements. Next-generation sequencing (NGS), performed on primary clinical samples, offers a promising alternative for analysis of the bacterial resistome. In this study, we describe the adaptation of a target-enrichment library preparation and NGS workflow for use on formalin-fixed, paraffin-embedded (FFPE) gastric biopsies to investigate both the *H. pylori* resistome and virulome. In total, 30 FFPE gastric biopsy samples were analyzed, all derived from patients infected with *H. pylori*, the majority of whom presented with gastritis or epigastric pain. The Agilent SureSelect XT protocol was modified for implementation on the Magis automated system, and sequencing was performed using the iSeq 100 platform. RNA probes targeting key genes associated with virulence (e.g., *cagA* and *vacA*), antibiotic resistance (e.g., *23S rRNA*, *16S rRNA*, *gyrA*, and *rpoB*), and multilocus sequence typing (MLST) were employed. The resulting sequence data were compared to those obtained from cultured *H. pylori* strains isolated from the same patients. Mutations in *23S rRNA* linked to macrolide resistance, those in the quinolone resistance-determining region of *gyrA* associated with levofloxacin resistance, and those conferring rifamycin resistance were accurately detected. The MLST profiles generated through this method were consistent with those obtained via Sanger sequencing. Furthermore, the *cagA* gene, including EPIYA motifs, and *vacA* genotypes were reliably identified. This target-enrichment technique provides accurate access to the *H. pylori* resistome and virulome directly from FFPE biopsy specimens, representing a significant technological advancement.

**Keywords** Resistome, Virulome, FFPE, Gastric biopsy, NGS, *H. pylori*

The diagnosis of *Helicobacter pylori* infection is based on either non-invasive methods—such as serological testing, the urea breath test, or stool antigen detection—or invasive approaches, including histology, culture, polymerase chain reaction (PCR), and next-generation sequencing (NGS) techniques, which analyze gastric or duodenal biopsy specimens<sup>1</sup>. The choice between non-invasive and invasive diagnostic tests depends on the clinical context. Histological examination has long been regarded as the gold standard for diagnosing *H. pylori* infection<sup>1</sup>. It not only assesses the extent of gastric inflammation but also enables the classification of

<sup>1</sup>CHU de Bordeaux, CNR des Campylobacters et des Hélicobacters, Bordeaux, France. <sup>2</sup>Department of Pathology, CHU de Bordeaux, Bordeaux, France. <sup>3</sup>Department of Tumor Biology, CHU de Bordeaux, Bordeaux, France. <sup>4</sup>INSERM U1312, UMR BRIC-Team 4, Bordeaux, France. <sup>5</sup>Université de Bordeaux, 33000 Bordeaux, France. <sup>6</sup>CHU Pellegrin, Laboratoire de Bactériologie, CNR des Campylobacters et des Hélicobacters, Place Amélie Raba Léon, 33076 Bordeaux Cedex, France. ✉email: philippe.lehours@u-bordeaux.fr

lesions, particularly those that are ulcerative, metaplastic, dysplastic, or malignant, such as adenocarcinoma or mucosa-associated lymphoid tissue lymphoma. Histology is typically complemented by immunohistochemistry to detect *H. pylori* infection. This comprehensive diagnostic information is crucial for clinicians in the effective management of these infections. Biopsies submitted for histological examination require only fixation in formalin at room temperature, a straightforward and widely accessible procedure. However, although histology can provide a comprehensive diagnostic overview, it does not offer information on the antibiotic resistance profile of the infecting *H. pylori* strain. Although fluorescence in situ hybridization technology is used in a few countries to detect resistance<sup>2</sup>, it remains uncommon in routine clinical practice. As a result, clinicians often rely on empiric, or probabilistic, eradication strategies based on local resistance patterns, such as bismuth-containing quadruple therapy or concomitant therapy<sup>3,4</sup>.

When sending a gastric biopsy to a microbiology laboratory for *H. pylori* culture, specific and more stringent transport conditions are required to preserve bacterial viability. Ideally, the biopsy should be placed in a dedicated transport medium such as Portagerm Pylori, which allows for refrigerated transport at +4 °C within 48 h<sup>5</sup>. Alternatively, immediate freezing in liquid nitrogen or on dry ice in a sterile tube can be employed, although this approach necessitates a well-coordinated logistical framework. The use of physiological saline is not recommended, as it does not reliably maintain the viability of *H. pylori*<sup>1</sup>. Culturing *H. pylori* demands specialized expertise due to the organism's fragile nature and the requirement for selective culture media, some of which are commercially available. Despite these challenges, culture offers a key advantage: it enables antibiotic susceptibility testing, allowing clinicians to prescribe personalized eradication regimens based on the resistance profile of the strain<sup>6,7</sup>. This targeted approach is generally better tolerated than empirical, or probabilistic, treatments, leading to improved adherence and a reduced risk of premature discontinuation. Ultimately, this enhances treatment success rates. Despite their value, *H. pylori* culture and PCR testing are not routinely performed in many countries due to numerous obstacles. The fragility of the bacteria requires strict preanalytical conditions for transporting biopsies. *H. pylori* culture is difficult and requires a certain level of expertise. Access to commercial PCR kits for detecting *H. pylori* is not possible in many countries. The lack of reimbursement for this highly sensitive test is a major obstacle in many countries. As a result, many gastroenterologists are satisfied with a histological diagnosis, which has long been considered the gold standard. The main idea behind this project is to use these paraffin-embedded biopsies to provide clinicians with microbiological data enabling them, if they wish, to prescribe targeted antibiotic therapy for *H. pylori* infections.

As an alternative to culture, gastric biopsies can be analyzed using molecular biology techniques. *H. pylori* PCR most commonly targets the 23S *rRNA*, particularly the V-loop region, which harbors mutations associated with macrolide resistance at positions 2142 and 2143<sup>8</sup>. Several real-time PCR kits with excellent analytical performance are commercially available in many countries<sup>9,10</sup>. PCR is more sensitive than histology, which may underestimate 10–20% of infections<sup>11</sup>. However, its widespread use is hindered by limited reimbursement by national health systems, with only a few countries, such as France, currently covering its cost. NGS approaches using DNA extracted from gastric biopsies have also been developed and described by several research groups, including our own<sup>12,13,14</sup>. These methods enable comprehensive analysis of the bacterial resistome and, potentially, the virulome. Despite their advanced capabilities, the high cost and lack of reimbursement by healthcare systems remain major barriers to their broader implementation. Although PCR and NGS represent powerful tools in the modern diagnostic arsenal for *H. pylori* infection, both still require gastric biopsies to be sent to a microbiology laboratory. Unfortunately, in France—as in many other countries—clinicians often favor procedural simplicity and typically limit diagnostic evaluation to histological analysis alone.

The aim of this study was to evaluate the performance of the target enrichment followed by NGS amplification techniques previously described by our group<sup>14</sup> for characterizing the *H. pylori* resistome and virulome in fresh gastric biopsies. Specifically, we investigated whether this approach could be applied to DNA extracted from paraffin-embedded biopsies routinely sent to histology laboratories. In a cohort of 30 biopsies that were histologically positive for *H. pylori*, we demonstrated that this technique yields results comparable to those obtained from parallel biopsies collected from the same patients and analyzed in microbiology laboratories using real-time PCR and culture with antibiotic susceptibility testing.

## Results

### Global evaluation of sequencing depth and coverage

To evaluate our method using clinical specimens, we tested 30 samples that were all positive for *H. pylori* by real-time PCR, with cycle threshold (Ct) values ranging from 25.8 to 37 (Table 1; Supplementary Table 1). Although most samples demonstrated sufficient sequencing quality for downstream analyses, several exhibited suboptimal base depth and gene coverage, rendering the detection of resistance markers, characterization of virulence-associated genes, and phylogenetic analyses incomplete or impossible. Specifically, samples 6, 8, 10, 14, 17, 21, 23, 27, 28, and 30 failed to achieve complete characterization due to inadequate sequencing quality in 2 to 5 targeted regions. Correlation analysis between average sequencing depth and real-time PCR Ct values (Fig. 1) revealed that all samples with Ct values below 30.0 met the criterion of achieving a mean depth of at least 10× across all targeted regions (Supplementary Table 2). Notably, samples 11 and 18 displayed unexpectedly high sequencing quality despite their relatively late Ct values of 32.2 and 33.7, respectively. Overall, average sequencing depth across target regions decreased as *H. pylori* PCR Ct values increased (Fig. 1). A log–log linear regression model fitted to the data confirmed a significant negative association between Ct and average depth ( $p < 0.0001^{***}$ ), with an adjusted  $R^2$  of 0.66. Based on this model, we estimated a Ct cutoff of approximately 32.9, above which samples are unlikely to achieve an average sequencing depth of 10× across the targeted regions.

Another approach to assess the quality of our libraries involved characterizing their DNA composition. By tracking information at various stages of the mapping-based pipeline, we could determine whether sequencing reads were filtered out before mapping—primarily due to poor quality or insufficient length—or whether they

Sample N	Sex	Age	Previous eradication	Pathology, symptoms	<i>H. pylori</i> Ct	23S <i>rRNA</i> genotype determined by RT-PCR	AST resistance markers
1	Female	6	No	Anemia	28.7	A2142G or A2143G	Cla
2	Female	56	No	Gastritis	25.8	A2142G or A2143G	Cla
3	Female	46	Yes	Gastritis	28.7	A2142G or A2143G	Cla
4	Female	14	No	Gastritis	29.7	A2142G or A2143G	Cla, Lev
5	Female	9	No	Other	28.5	WT	Lev
6	Female	20	Yes	Gastritis	33.3	WT + A2142G or A2143G	
7	Female	30	No	Other	27.7	WT	Lev
8	Female	13	No	Gastritis	30.6	A2142C	Cla, Lev
9	Female	11	No	Emesis	29.1	A2142G or A2143G	Cla
10	Male	3	No	GERD	34.1	A2142G or A2143G	Cla, Lev
11	Male	22	Yes	Gastritis	32.2	WT	Lev
12	Female	57	Yes	Gastritis	28.1	A2142G or A2143G	Cla
13	Female	14	No	Gastritis	26.3	WT	Lev
14	Male	63	Yes	Gastritis	31.4	WT	Lev
15	Male	1	No	Other	28.1	WT	
16	Male	53	Yes	Gastritis	29.5	A2142G or A2143G	Cla
17	Male	80	No	Ulcers	32.4	A2142G or A2143G	Cla, Lev
18	Male	1	Yes	Ulcers	33.7	WT + A2142G or A2143G	
19	Male	68	Yes	Epigastralgia	30	WT	Lev
20	Male	13	No	Other	27.9	WT	
21	Female	61	Yes	Epigastralgia	33.9	WT	
22	Male	61	No	Gastritis	29.3	A2142G or A2143G	Cla, Lev
23	Male	32	No	Gastritis	37	A2142G or A2143G	Cla
24	Male	65	No	Other	30.8	WT	
25	Male	18	Yes	Gastritis	29.1	WT	
26	Male	65	Yes	Gastritis	28.6	A2142G or A2143G	Cla, Lev
27	Female	40	Yes	Gastritis	34.9	A2142G or A2143G	
28	Male	87	No	Gastritis	28.7	WT	
29	Female	39	Yes	Gastritis	29.1	A2142G or A2143G	Cla
30	Female	71	No	Other	32.4	WT	

**Table 1.** Description of included cases. GERD, gastroesophageal reflux disease; Cla, clarithromycin; Lev, levofloxacin; AST, antimicrobial susceptibility testing.

mapped to the human genome, to *H. pylori* (“on-target”), or remained unmapped (Fig. 2). Samples with a higher *H. pylori* colonization, indicated by Ct values between 25.8 and 32.9 (24 samples), exhibited a significantly higher percentage of reads mapped to the *H. pylori* reference genome ( $14 \pm 4\%$ ) compared to samples with Ct values above 33, which showed only  $3\% \pm 1\%$  mapped reads (Fig. 2A). All samples with over 10,000 reads mapped to *H. pylori* demonstrated excellent sequencing quality (Supplementary Fig. 1). Although gene coverage correlated with the number of reads, it did not always reflect read quality. Several libraries were contaminated with human and unidentified DNA. For example, sample 30, which had one of the highest Ct values for *H. pylori*, contained 62% human DNA but only 1% of reads mapped to *H. pylori*. This likely indicates non-specific capture of unwanted DNA by probes that hybridize to conserved regions present in other bacteria—such as the *16S* or *23S rRNA* operons—or to the human genome. Additionally, some libraries, such as samples 17 and 23, showed a higher proportion of short fragments ( $< 50$  bp) (Fig. 2A). This phenomenon may be caused by the presence of primer dimers, which typically arise when the targeted DNA content in the sample is low.

A notable limitation of this approach is that a proportion of PCR positive samples, particularly those with higher Ct values, could not be fully characterized due to insufficient sequencing depth and coverage of all targeted regions. This likely reflects the limited amount of *H. pylori*-specific DNA relative to host background DNA, as well as potential library preparation artifacts such as probe homodimers.

### Detection of clarithromycin resistance markers

Mutations in the *23S rRNA* gene identified via target enrichment were compared to those detected by real-time PCR on fresh gastric biopsies. The concordance between the two methods was good in 25 of the 30 samples tested (83.3%), with all genotypes accurately identified (Table 2). The predominant mutation detected was A2143G, and the sole A2142C mutation (sample 8) was also correctly identified. However, base depth was insufficient in samples 6, 10, 21, and 23—each with Ct values ranging from 33.3 to 37 in DNA extracted from FFPE tissue (Table 1; Supplementary Table 1). A mixed population of wild-type and mutant *H. pylori* was detected in samples 18 and 27, with the mutant alleles representing 70% and 90% of the called bases, respectively. Notably, for sample 27, no mixed population was identified by AST, real-time PCR on fresh gastric biopsies, or WGS of

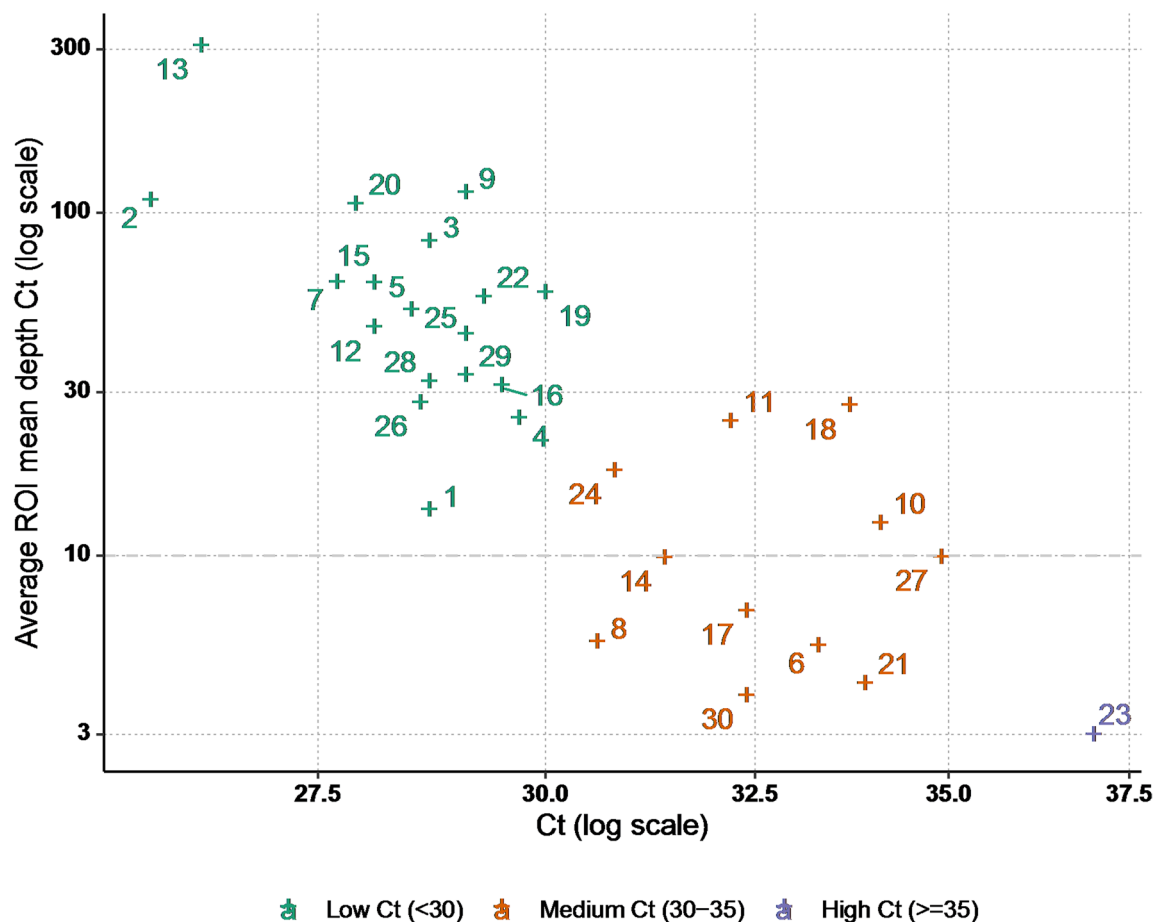


**Fig. 1.** Correlation between average sequencing depth across targeted regions and *H. pylori* PCR Ct values.

the corresponding *H. pylori* isolate. This suggests a heterogeneous distribution of the clarithromycin-resistant subpopulation within the patient's stomach, detectable only in the FFPE biopsy samples. When compared with AST results, the correlation with target enrichment data from FFPE samples was good. In sample 6, which had insufficient base depth by target enrichment, and sample 18, mixed populations were confirmed both in vitro, by real-time PCR on gastric DNA, and by WGS of the corresponding *H. pylori* strain.

#### Detection of levofloxacin resistance markers

Mutations in the quinolone resistance-determining region (QRDR) of the *gyrA* gene identified via target enrichment were compared with those detected by WGS of the corresponding *H. pylori* strains (Table 3). The correlation was good in 20 of the 30 samples (66.7%). Insufficient base depth was observed in nine samples (samples 6, 8, 14, 17, 21, 23, 27, 28, and 30), all but one (sample 28) testing positive by *H. pylori* real-time PCR with Ct values above 30 cycles. In sample 29, a mixed population was detected by AST and WGS, whereas target enrichment identified only a wild-type population. This suggests a heterogeneous distribution of the levofloxacin-resistant subpopulation in the patient's stomach, detectable only by culture, despite the resistant bacteria constituting approximately 10% of the total population. The mutations associated with levofloxacin resistance identified were D91G (one sample with mixed infection), D91N (five samples, including one mixed infection), N87K (three samples), and N87I (three samples).

#### Detection of rifabutin and tetracycline resistance markers

Insufficient base depth for the *rpoB* gene was observed in the same nine samples as for *gyrA* (samples 6, 8, 14, 17, 21, 23, 27, 28, and 30). A H540Y mutation in *rpoB* was identified by target enrichment in sample 12; however, this mutation was not confirmed by either AST or WGS of the corresponding *H. pylori* isolate (Suppl Table 3). This discrepancy may again reflect a heterogeneous distribution of the resistant subpopulation within the patient's stomach, detectable only in FFPE samples. No other mutations were detected in the remaining samples, consistent with the NGS results from the cultured *H. pylori* strains. No resistance markers for tetracycline were identified in any of the 30 samples (data not shown), as expected, since no tetracycline-resistant *H. pylori* isolates were included in this study. This outcome supports the reliability of sequencing for genes involved in tetracycline and rifampicin resistance. The only exceptions were the nine samples (6, 8, 14, 17, 21, 23, 27, 28, and 30) that exhibited poor sequencing quality across these targeted regions (Suppl Tables 1 and 4).

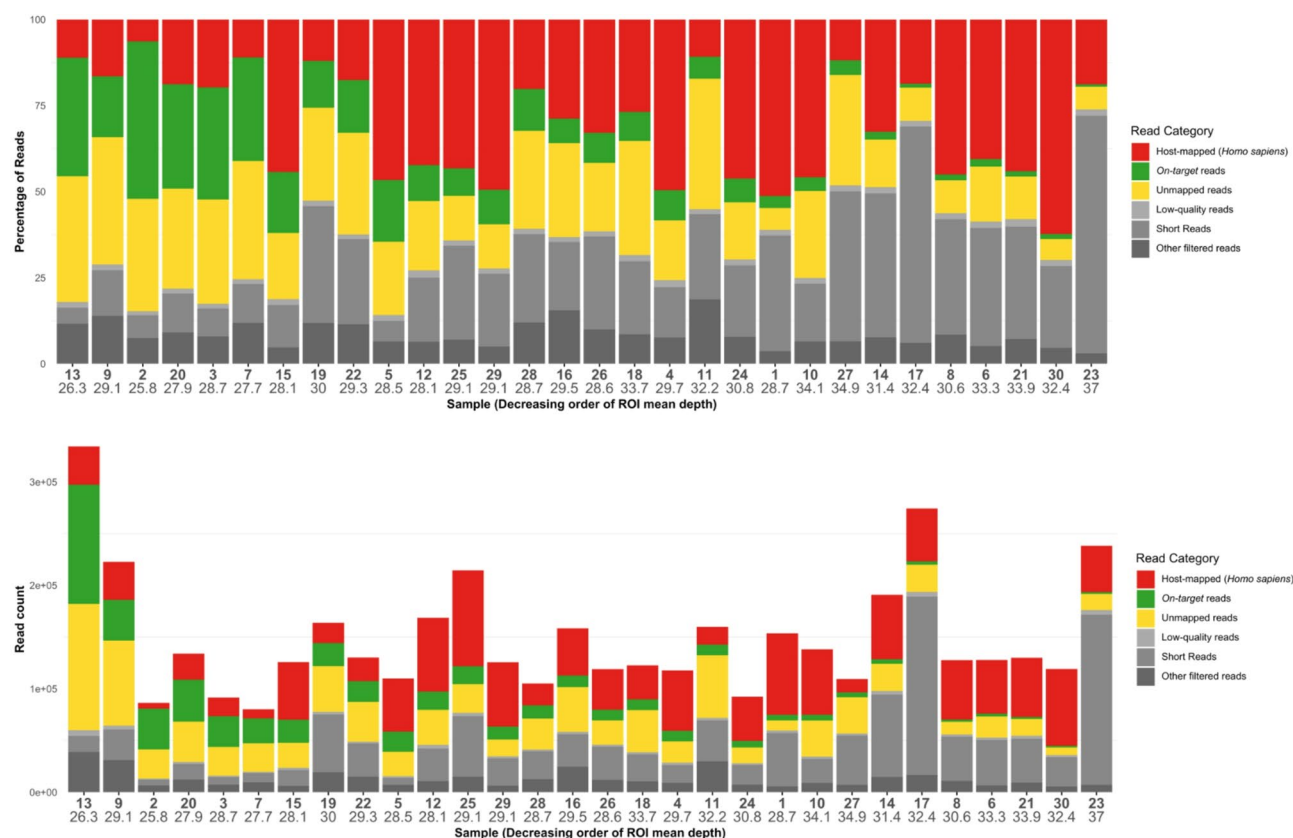


**Fig. 2.** Distribution of sequencing reads by category, illustrating sample quality.

### Virulence typing

The *cagA* gene was detected by target enrichment in 13 of the 14 *cagA*-positive samples (92.9%) identified by WGS of the corresponding strains (Table 4). Except for sample 30, the assembly quality of *cagA* sequences was sufficient to detect the EPIYA phosphorylation motifs in all other 12 samples. The determination of the number of EPIYA-C motifs was good, with the exception of sample 20, for which target enrichment identified two C motifs, whereas WGS of the *H. pylori* strain detected only one. Regarding *vacA* genotypes, the correlation between target enrichment and WGS was good in 22 of the 30 samples (73.3%). No genotype prediction was possible for samples 6, 21, 23, and 27 due to insufficient assembly length. For samples 10, 30, and 17, only the s1, i1, and i2 genotypes were identified, respectively. In sample 1, which was classified as s1i2m2 by WGS, the m genotype was not detected by target enrichment.

### MLST of clinical samples

Geographic attribution of samples was determined from the concatenated sequences of the *H. pylori* typing scheme using STRUCTURE and a database of annotated sequences from PubMLST. The results obtained by WGS of *H. pylori* were compared with those from target enrichment (Table 5). The correlation between the two methods was good. Most biopsies (16 of 30, 53.3%) contained hpEurope *H. pylori* strains. Seven biopsies (23.3%) contained hpEurope/hpAfrica1 hybrids, with hpAfrica1 strains representing between 11 and 86% of the profile according to WGS results, or an estimated 7% to 75% by target enrichment. Six cases (20%) were attributed solely to hpAfrica1, and one remaining sample was identified as an hpEurope/hpEAsia hybrid. A minor discrepancy was observed for sample 10, which was classified as hpEurope by target enrichment but identified as an hpEurope/hpAfrica1 hybrid by WGS of the strain. Lastly, the geographic cluster for sample 23 could not be determined due to insufficient sequencing quality in the relevant regions of the typing scheme.

### Discussion

In this work, we demonstrate that target enrichment followed by NGS amplification of DNA extracted from FFPE biopsies enables comprehensive analysis of the *H. pylori* resistome and virulome. The concordance between NGS results and those obtained in vitro (PCR and antibiogram) on fresh biopsies was excellent.

Compared with our previous study on fresh biopsies<sup>14</sup>, coverage and read depth were improved. We also obtained analyzable results from DNA extracted from FFPE biopsies, positive by PCR, with Ct values close to 30. The fragmentation of DNA caused by formalin fixation in FFPE blocks appears to be an advantage for our technique, which relies on small RNA probes that can bind more effectively to degraded bacterial genomic DNA.



Sample N	Phenotypical susceptibility observed by AST and clarithromycin MIC	Observed mutation by RT-PCR	Observed mutation by WGS of strain	Observed mutation by target enrichment of paraffin-embedded biopsy samples
1	Resistant (12 mg/L)	A2142G or A2143G	A2143G (100%)	A2143G (100%)
2	Resistant (16 mg/L)	A2142G or A2143G	A2143G (100%)	A2143G (100%)
3	Resistant (24 mg/L)	A2142G or A2143G	A2143G (100%)	A2143G (100%)
4	Resistant (12 mg/L)	A2142G or A2143G	A2143G (100%)	A2143G (100%)
5	Susceptible (0.032 mg/L)	WT	WT	WT
6	Susceptible-resistant mix (0.25 mg/L; 16 mg/L)	WT + A2142G or A2143G	WT + A2143G (70%)	Insufficient base depth
7	Susceptible (0.016 mg/L)	WT	WT	WT
8	Resistant (> 256 mg/L)	A2142C	A2142C (100%)	A2142C (100%)
9	Resistant (4 mg/L)	A2142G or A2143G	A2143G (100%)	A2143G (100%)
10	Resistant (8 mg/L)	A2142G or A2143G	A2143G (100%)	Insufficient base depth
11	Susceptible (< 0.016 mg/L)	WT	WT	WT
12	Resistant (1 mg/L)	A2142G or A2143G	A2143G (100%)	A2143G (100%)
13	Susceptible (0.016 mg/L)	WT	WT	WT
14	Susceptible (0.016 mg/L)	WT	WT	WT
15	Susceptible (< 0.016 mg/L)	WT	WT	WT
16	Resistant (3 mg/L)	A2142G or A2143G	A2143G (100%)	A2143G (100%)
17	Resistant (256 mg/L)	A2142G or A2143G	A2142G (100%)	A2142G (100%)
18	Susceptible-resistant mix (0.25 mg/L; 16 mg/L)	WT + A2142G or A2143G	WT + A2143G (90%)	WT + A2143G (90%)
19	Susceptible (0.032 mg/L)	WT	WT	WT
20	Susceptible (0.047 mg/L)	WT	WT	WT
21	Susceptible (< 0.016 mg/L)	WT	WT	Insufficient base depth
22	Resistant (12 mg/L)	A2142G or A2143G	A2143G (100%)	A2143G (100%)
23	Resistant (16 mg/L)	A2142G or A2143G	A2142G (100%)	Insufficient base depth
24	Susceptible (< 0.016 mg/L)	WT	WT	WT
25	Susceptible (0.016 mg/L)	WT	WT	WT
26	Resistant (12 mg/L)	A2142G or A2143G	A2143G (100%)	A2143G (100%)
27	Resistant (16 mg/L)	A2142G or A2143G	A2143G (100%)	WT + A2143G (70%)
28	Susceptible (0.125 mg/L)	WT	WT	WT
29	Resistant (3 mg/L)	A2142G or A2143G	A2143G (100%)	A2143G (100%)
30	Susceptible (< 0.016 mg/L)	WT	WT	WT

**Table 2.** 23S *rRNA* mutations linked to clarithromycin resistance detected among studied samples. WT, wild-type. Insufficient base depth, Base depth < 5 at any mutation site.

The sensitivity of target enrichment on FFPE samples is limited to those positive by PCR using our in-house assay with Ct values up to 30 cycles. Any laboratory wishing to implement this strategy will need to validate the detection limit based on their own routine PCR format.

In two cases included in this study, only the susceptible or resistant population were detected by target enrichment, unlike the results from in vitro testing. This discrepancy may be due to the fact that biopsies for histology and bacteriology not being taken from exactly the same anatomical site. In fact, more biopsies are taken for histological diagnosis than for bacteriology. The area of the mucosa covered by histology is therefore larger (a minimum of 5 biopsies is recommended), which increases the chances of identifying mixed infections in patients infected with strains with different resistance profiles and distributed heterogeneously in the gastric mucosa. Previous studies have shown that some patients may harbor mixed infections with respect to certain antibiotic resistance or virulence markers<sup>15,16</sup>. Our NGS approach on FFPE biopsies may therefore offer an advantage in detecting these mixed infections. The discrepancy we observed in a biopsy where 20% of a potentially rifamycin-resistant population was detected is particularly notable. It is likely that rifabutin treatment in this patient would not have been effective. This finding supports the recommendation to collect multiple biopsies from different anatomical sites to capture more accurately the bacterial diversity present. For levofloxacin, as our approach did not detect heteroresistance in sample 29, in which resistant bacteria represented approximately 10% of the population, it may suggest limited sensitivity for minority variants.

Other groups have described alternative NGS approaches applicable to DNA extracted from FFPE biopsies<sup>13</sup>. However, our study has the advantage of comparing target enrichment results with those obtained by real-time PCR, culture, AST, and WGS on all included biopsies.

Compared with commercially available kits such as American Molecular<sup>17</sup> or GenoScreen Deeplex Help (<https://www.deeplex.com/deeplex-help/>), our probe design offers greater adaptability, allowing the addition of resistance or virulence markers as new genomic markers are validated. For example, once markers for *H. pylori* resistance to amoxicillin or metronidazole are confirmed, corresponding probes can be incorporated. Our probe

Sample N	Phenotypical susceptibility observed by AST and levofloxacin MIC	Observed mutation by WGS of strain	Observed mutation by target enrichment of paraffin-embedded biopsy samples
1	Susceptible (0.064 mg/L)	WT	WT
2	Susceptible (0.064 mg/L)	WT	WT
3	Susceptible (0.125 mg/L)	WT	WT
4	Resistant (> 32 mg/L)	N87I (100%)	N87I (100%)
5	Resistant (3 mg/L)	D91N (100%)	D91N (100%)
6	Susceptible (0.094 mg/L)	WT	Insufficient base depth
7	Resistant (2 mg/L)	D91N (100%)	D91N (100%)
8	Resistant (> 32 mg/L)	N87K (100%)	Insufficient base depth
9	Susceptible (0.250 mg/L)	WT	WT
10	Resistant (> 32 mg/L)	N87K (100%)	N87K (100%)
11	Resistant (32 mg/L)	N87K (100%)	N87K (100%)
12	Susceptible (0.094 mg/L)	WT	WT
13	Resistant (1.5 mg/L)	WT + D91G (90%)	WT + D91G (90%)
14	Resistant (12 mg/L)	D91N (100%)	Insufficient base depth
15	Susceptible (0.190 mg/L)	WT	WT
16	Susceptible (0.190 mg/L)	WT	WT
17	Resistant (32 mg/L)	D91N (100%)	Insufficient base depth
18	Susceptible (0.125 mg/L)	WT	WT
19	Resistant (> 32 mg/L)	N87I (100%)	N87I (100%)
20	Susceptible (0.250 mg/L)	WT	WT
21	Susceptible (0.047 mg/L)	WT	Insufficient base depth
22	Resistant (> 32 mg/L)	N87I (100%)	N87I (100%)
23	Susceptible (0.125 mg/L)	WT	Insufficient base depth
24	Susceptible (0.094 mg/L)	WT	WT
25	Susceptible (0.190 mg/L)	WT	WT
26	Resistant (8 mg/L)	D91N (100%)	D91N (100%)
27	Susceptible (0.190 mg/L)	WT	Insufficient base depth
28	Susceptible (0.125 mg/L)	WT	Insufficient base depth
29	Susceptible-resistant mix (0.25 mg/L; 6 mg/L)	WT + D91N (10%)	WT
30	Susceptible (0.190 mg/L)	WT	Insufficient base depth

**Table 3.** *GyrA* mutations linked to levofloxacin resistance detected among studied samples. WT, wild-type.

design has been updated from the version described by Gillet et al.<sup>14</sup>, notably by including the determination of the *htrA* genotype, recently identified by Prof. S. Backert's team as an important virulence marker for *H. pylori*<sup>18,19</sup>. The resistome analysis on FFPE biopsies was highly effective, including accurate determination of the number of repeats of the C motif in *CagA* EPIYA phosphorylation sites<sup>20</sup>. The determination of *vacA* genotypes was also accurate; however, as with fresh biopsies, probe adjustments may be needed to improve coverage of the m2 genotype. The absence of patients with pre-neoplastic lesions or adenocarcinoma in our cohort likely explains why all patients infected with a *cagA*-positive strain had a wild-type *htrA* genotype. Additionally, the number of strains with C motif repeats was low.

It would now be valuable to test routinely a larger number of biopsies in collaboration with clinicians and pathologists to further demonstrate the clinical utility of these NGS results. Our center offers this technique on FFPE blocks specifically for cases of eradication failure, particularly in patients where successful eradication would provide significant clinical benefit. The turnaround time for this approach is approximately one week. Patients with ulcers, pre-neoplastic lesions, mucosa-associated lymphoid tissue lymphoma, or adenocarcinoma represent particularly relevant candidates for this new technology. With a view to routine use of the strategy proposed in our study, obvious precautions will need to be taken to avoid any cross-contamination between samples. In addition to these potential contamination risks, another potential challenge that could limit the adoption of NGS is its use in countries with limited economic resources. However, partnerships with expert laboratories such as ours, provide solutions for the routine application of this new approach.

A limitation of our approach is that approximately 30% of FFPE samples had insufficient coverage for some targets. The inherent fragmentation of FFPE-derived DNA may bias detection toward smaller genomic regions, potentially underrepresenting larger or more complex loci. Rare genotypes or low-frequency variants, such as certain *htrA* or *vacA* alleles, may therefore be under-detected. The limited performance of target enrichment in low-bacterial-load FFPE samples, also impacts resistance detection, virulence typing, and strain attribution. Finally, the absence of patients with pre-neoplastic lesions or adenocarcinoma also limits the generalizability of the findings to broader clinical populations.

Sample N	Observed <i>cagA</i> genotype motifs by WGS of strain	Observed <i>cagA</i> genotype by target enrichment of paraffin-embedded biopsy	Observed <i>vacA</i> genotype by WGS of strain	Observed <i>vacA</i> genotype by target enrichment of paraffin-embedded biopsy samples
1	Positive, ABC	Positive, BC	s1/i2/m2	s1/i2/m?
2	Positive, B'CC	Positive, B'CC	s1/i2/m2	s1/i2/m2
3	Positive, ABC	Positive, ABC	s1/i1/m1	s1/i1/m1
4	Negative	Negative	s1/i1/m1	s1/i1/m1
5	Positive, ABC	Positive, ABC	s1/i1/m1	s1/i1/m1
6	Positive, ABC	Negative	s1/i1/m1	Insufficient coverage
7	Positive, ABC	Positive, ABC	s1/i1/m1	s1/i1/m1
8	Positive, ABC	Positive, no motif	s1/i2/m2	s1/i2/m2
9	Negative	Negative	s2/i2/m2	s2/i2/m2
10	Negative	Negative	s1/i1/m2	s1/i?/m?
11	Negative	Negative	s2/i2/m2	s2/i2/m2
12	Negative	Negative	s2/i2/m2	s2/i2/m2
13	Positive, ABC	Positive, ABC	s1/i1/m1	s1/i1/m1
14	Positive, AB'C	Positive, AC	s1/i1/m1	s1/i1/m1
15	Negative	Negative	s2/i2/m2	s2/i2/m2
16	Negative	Negative	s2/i2/m2	s2/i2/m2
17	Negative	Negative	s2/i2/m2	s?/i2/m?
18	Negative	Negative	s2/i2/m2	s2/i2/m2
19	Positive	Positive, no motif	s1/i1/m1	s1/i1/m1
20	Positive, ABC	Positive, ABCC	s1/i1/m1	s1/i1/m1
21	Negative	Negative	s2/i2/m2	Insufficient coverage
22	Negative	Negative	s2/i2/m2	s2/i2/m2
23	Negative	Negative	s2/i2/m2	Insufficient coverage
24	Negative	Negative	s2/i2/m2	s2/i2/m2
25	Positive, AB	Positive, AB	s1/i1/m1	s1/i1/m1
26	Negative	Negative	s2/i2/m2	s2/i2/m2
27	Negative	Negative	s2/i2/m2	Insufficient coverage
28	Positive, AB'C	Positive, AB'C	s1/i1/m1	s1/i1/m1
29	Negative	Negative	s1/i1/m2	s1/i1/m2
30	Positive, AB'C	Positive, no motif	s1/i1/m1	s?/i1/m?

**Table 4.** Observed *cagA* and *vacA* genotypes from strain and paraffin-embedded sequencing. ?, undetermined.

Nevertheless, the use of target enrichment on DNA extracted from FFPE biopsies constitutes a promising approach with clear advantages. It offers clinicians a promising tool to implement targeted eradication strategies without requiring changes to their current clinical practices.

Methods  
Biopsy

In total, 30 gastric biopsies submitted to the pathology department of Bordeaux University Hospital were analyzed. These samples were collected between 2021 and 2024 from 13 men and 17 women, with a median age of 38.6 ± 26.5 years (Table 1). The patients presented with various clinical conditions, including gastritis (n = 17), ulcers (n = 2), epigastric pain (n = 2), anemia (n = 1), emesis (n = 1), gastroesophageal reflux disease (n = 1), and other disorders (n = 6) (Table 1). *H. pylori* infection was confirmed in all cases by immunohistochemical staining using the Leica Bond III automated immunostainer protocol (Leica IHC-F, Leica Microsystems SA, Nanterre, France), with detection performed using the ULC3R clone antibody at a 1:50 dilution. In addition, all patients were confirmed positive for *H. pylori* through culture and real-time PCR analysis of fresh gastric biopsies sent in parallel to the National Reference Center for Campylobacters and Helicobacters (NRCCH). The real-time PCR used for *H. pylori* detection coupled with the main mutations associated with resistance to clarithromycin was previously described<sup>21</sup>. It corresponds to ready-to-use PCR microwell strips used on LightCycler® 480. These PCR microwell strips are available for purchase from Eurogentec (Liège, Belgium).

Bacterial culture

In total, 30 *H. pylori* isolates, corresponding to the same patients whose formalin-fixed paraffin-embedded (FFPE) biopsies were analyzed by target enrichment, were obtained from fresh gastric biopsies sent to the NRCCH. The biopsies were initially cultured on in-house prepared blood agar supplemented with antibiotics and incubated under microaerobic conditions in a controlled workstation (Baker Ruskinn, Concept Ruskinn, Bridget, UK) at 36 °C for up to 10 days. Antimicrobial susceptibility testing (AST) data were collected for all isolates. AST



Sample N	Assigned geographic profile by WGS of strain	Assigned geographic profile by target enrichment of paraffin-embedded biopsy samples
1	hpEurope	hpEurope
2	hpEurope (90%), hpAfrica (10%)	hpEurope (90%), hpAfrica1 (10%)
3	hpAfrica1	hpAfrica1
4	hpAfrica1	hpAfrica1
5	hpAfrica1	hpAfrica1
6	hpAfrica (85%), hpEurope (15%)	hpAfrica1 (75%), hpEurope (25%)
7	hpEurope	hpEurope
8	hpEurope	hpEurope
9	hpEurope (75%), hpAfrica1 (25%)	hpEurope (75%), hpAfrica1 (25%)
10	hpEurope	hpEurope (75%), hpAfrica1 (25%)
11	hpEurope	hpEurope
12	hpEurope	hpEurope
13	hpEurope (55%), hpAfrica1 (45%)	hpEurope (66%), hpAfrica1 (33%)
14	hpEurope	hpEurope
15	hpAfrica1	hpAfrica1
16	hpEurope	hpEurope
17	hpEurope	hpEurope
18	hpEurope (85%), hpAfrica1 (15%)	hpEurope (80%), hpAfrica1 (20%)
19	hpAfrica1	hpAfrica1
20	hpEAsia (45%), hpEurope (55%)	hpEAsia1 (55%), hpEurope (45%)
21	hpEurope	hpEurope
22	hpEurope (50%), hpAfrica1 (50%)	hpEurope (55%), hpAfrica1 (45%)
23	hpEurope	Insufficient coverage over genes
24	hpEurope	hpEurope
25	hpAfrica1	hpAfrica1
26	hpEurope (80%), hpAfrica1 (20%)	hpEurope (75%), hpAfrica1 (25%)
27	hpEurope	hpEurope
28	hpEurope	hpEurope
29	hpEurope	hpEurope
30	hpEurope	hpEurope

**Table 5.** Observed MLST profiles from strain and paraffin-embedded sequencing.

was performed on Mueller–Hinton agar supplemented with 10% sheep blood and freshly prepared globular extract. Minimum inhibitory concentrations (MICs) for clarithromycin and levofloxacin were determined using Etest® strips (bioMérieux), with breakpoint values established according to the guidelines of the French Microbiology Society’s AntibioGram Committee (CA-SFM/EUCAST) (CA-SFM / EUCAST: Société Française de Microbiologie Ed; 2024: p.1–177). MICs for clarithromycin, levofloxacin, rifampicin, and tetracycline were independently evaluated by two readers. Quality control was maintained using the *H. pylori* reference strain CCUG 17874.

**Whole-genome sequencing (WGS) of *H. pylori* strains cultured from gastric biopsies**

All 30 *H. pylori* isolates underwent WGS and AST. DNA extraction was performed using a combination of mechanical disruption (bead-beating), enzymatic digestion, and chemical lysis on Revvity’s Chemagic Prime instrument. Library preparation was conducted with Illumina’s DNA Prep kit utilizing Tecan’s DreamPrep NGS automation system, followed by sequencing on the Illumina NovaSeq 6000 platform. Bioinformatic analysis was carried out according to the pipeline described in our previous study, with the exception that genome assembly was performed using NCBI’s SKESA v2.5.1<sup>22</sup>. An additional annotation step was included to extract genomic sequences of the *cagA* and *vacA* genes using Prokka v1.14.5<sup>23</sup>.

**Probe design for target enrichment**

An RNA probe library comprising 13,245 probes of 120 nucleotides each, totaling 108 kbp, was designed by Agilent (Santa Clara, CA, USA). This probe library enables the detection of genomic mutations associated with antimicrobial resistance to clarithromycin (23S *rRNA*), levofloxacin (*gyrA*), rifampicin (*rpoB*), and tetracycline (16S *rRNA*) (Table 6)<sup>14</sup>. In addition, the library targets all genomic regions commonly used in the *H. pylori* multilocus sequence typing (MLST) scheme, as described by Falush et al.<sup>24,25</sup>. Probe design can be ordered from Agilent by referring to our laboratory.

Gene	Mutations	Associated resistance
<i>16S rRNA</i>	AGA926-928TTC, AGA926-928ATC, AGA926-928TTA, AGA926-928TGC, AGA926-928AGC, AGA926-928ATA	Tetracycline
<i>23S rRNA</i>	A2142C, A2142G, A2142T, A2143C, A2143G	Clarithromycin
QRDR ( <i>gyrA</i> )	N87K, N87I, N87Y, A88P, A88V, D91G, D91N, D91Y	Levofloxacin
<i>rpoB</i>	L525I, L525P, S526T, Q527H, Q527K, Q527R, F528E, D530A, D530E, D530G, D530N, D530V, T539A, H540C, H540N, H540Y, S545L, L547E, I586N, I586L, T588NL	Rifamycin

**Table 6.** List of mutations associated with resistance to primary antibiotics.

### Automated capture-based library preparation

Most steps of the SureSelectXT workflow were automated using Agilent's MagnisDx library preparation system, covering the process from enzymatic fragmentation to hybridized library capture. DNA extracted from FFPE biopsy samples using the QIAamp DNA FFPE Tissue Kit, was normalized to 100 ng in a 14 µL input volume. The size of the DNA extracted from the FFPE samples ranged from 200 to 1000 bp. Following Agilent's guidelines, enzymatic fragmentation was performed for 20 min for high-quality DNA. The protocol included 18 pre-capture PCR cycles and 24 post-capture PCR cycles.

### NGS short-read sequencing

The final library fragment size distribution and molarity were assessed using Agilent's TapeStation 4150 system with the High Sensitivity D1000 assay. A 2 µL aliquot of the library was diluted tenfold, mixed with 2 µL of High Sensitivity D1000 Sample Buffer, and normalized to an equimolar concentration of 0.125 nM. A total of 20 µL of this final mixture was then prepared for multiplex sequencing, which was carried out on the Illumina iSeq 100 sequencer (San Diego, CA, USA) with a sequencing read length of 2 × 150 base pairs and paired-end sequencing, at the NRCCH.

### Bioinformatics workflow

Raw sequencing reads were initially mapped to the human genome using Bowtie2 v2.4.5 with the Homo sapiens GRCh38 reference assembly. Unmapped reads were subsequently trimmed and cleaned using fastp v0.23.4. To reduce false positives, a deduplication step exploiting duplex metabarcoding of inserts was applied to generate consensus sequences. These processed reads were then aligned to the *H. pylori* reference genome J99 (assembly ASM98269v1) using Bowtie2. Consensus sequences for all targeted regions were extracted with FreeBayes v1.3.6 and BCFtools v1.19, with a minimum base depth required of 5X. A custom bioinformatics pipeline was then employed on these consensus sequences to detect genomic resistance markers and characterize the bacterial resistome.

Concurrently, a de novo assembly was performed using NCBI's SKESA v2.5.1 to reconstruct complete sequences of the *cagA* and *vacA* genes. Sequences corresponding to the MLST scheme were concatenated and analyzed with STRUCTURE v2.3.4 to assign each sample to a defined population cluster. These sequences were then compared against the continuously updated allele sequence database available on PubMLST. Phylogenetic trees were generated using RAXML-NG v1.2.2 with the GTR + Gamma substitution model. Finally, a set of in-house scripts was developed to integrate all analysis outputs, generate PDF and HTML reports, and produce circular genome visualizations using the Circos graphic library v0.69–9. FastQC v0.12.1 and QUAST v5.2.0 are used to assess mapping and assembly quality respectively.

### Statement

All diagnostic methods were performed routinely in accordance with relevant guidelines and regulations. All patients were investigated in a hospital setting, according to good clinical practices. In this routine process, consent for the endoscopic procedure and biopsy collection is always provided and kept in the patient's medical record.

### Data availability

Raw sequencing data generated using the target-enrichment library preparation method, along with whole-genome sequencing data of \*H. pylori\* strains, are available in the European Nucleotide Archive (ENA) under project number PRJEB85970.

Received: 4 June 2025; Accepted: 7 October 2025

Published online: 13 November 2025

### References

- Megraud, F. & Lehours, P. Helicobacter pylori detection and antimicrobial susceptibility testing. *Clin. Microbiol. Rev.* **20**, 280–322 (2007).
- Yilmaz, O. et al. Detection of Helicobacter pylori and determination of clarithromycin susceptibility using formalin-fixed, paraffin-embedded gastric biopsy specimens by fluorescence in situ hybridization. *Helicobacter* **12**, 136–141 (2007).
- Malfertheiner, P. et al. Helicobacter pylori eradication with a capsule containing bismuth subcitrate potassium, metronidazole, and tetracycline given with omeprazole versus clarithromycin-based triple therapy: A randomised, open-label, non-inferiority, phase 3 trial. *Lancet* **377**, 905–913 (2011).

4. Malfertheiner, P. et al. Management of *Helicobacter pylori* infection: The Maastricht VI/Florence consensus report. *Gut* <https://doi.org/10.1136/gutjnl-2022-327745> (2022).
5. Heep, M., Scheibl, K., Degrell, A. & Lehn, N. Transport and storage of fresh and frozen gastric biopsy specimens for optimal recovery of *Helicobacter pylori*. *J. Clin. Microbiol.* **37**, 3764–3766 (1999).
6. Delchier, J.-C. et al. Efficacy of a tailored PCR-guided triple therapy in the treatment of *Helicobacter pylori* infection. *Med Mal Infect* **50**, 492–499 (2020).
7. Amiot, A. et al. 14-day tailored PCR-guided triple therapy versus 14-day non-Bismuth concomitant quadruple therapy for *Helicobacter pylori* eradication: A multicenter, open-label randomized noninferiority controlled trial. *Helicobacter* **29**, e13076 (2024).
8. Occhialini, A. et al. Macrolide resistance in *Helicobacter pylori*: Rapid detection of point mutations and assays of macrolide binding to ribosomes. *Antimicrob. Agents Chemother.* **41**, 2724–2728 (1997).
9. Jehanne, Q., Bénéjat, L., Mégraud, F., Bessède, E. & Lehours, P. Evaluation of the Allplex™ *H. pylori* and ClariR PCR Assay for *Helicobacter pylori* detection on gastric biopsies. *Helicobacter* **25**, e12702 (2020).
10. Mégraud, F., Bénéjat, L., Ontsira Ngoyi, E. N. & Lehours, P. Molecular approaches to identify *Helicobacter pylori* antimicrobial resistance. *Gastroenterol. Clin. North Am.* **44**, 577–596 (2015).
11. Bénéjat, L., Ducournau, A., Lehours, P. & Mégraud, F. Real-time PCR for *Helicobacter pylori* diagnosis. The best tools available. *Helicobacter* **23**, e12512 (2018).
12. Argueta, E. A., Alsamman, M. A., Moss, S. F. & D'Agata, E. M. C. Impact of antimicrobial resistance rates on eradication of *Helicobacter pylori* in a US population. *Gastroenterology* **160**, 2181–2183.e1 (2021).
13. Herzlinger, M. et al. *Helicobacter pylori* antimicrobial resistance in a pediatric population from the New England Region of the United States. *Clin. Gastroenterol. Hepatol.* **21**, 3458–3460.e2 (2023).
14. Gillet, L. et al. Resistome and virulome determination in *Helicobacter pylori* using next-generation sequencing with target-enrichment technology. *Microbiol Spectr* <https://doi.org/10.1128/spectrum.03298-24> (2025).
15. Ben Mansour, K. et al. Multiple and mixed *Helicobacter pylori* infections: Comparison of two epidemiological situations in Tunisia and France. *Infect Genet. Evol* **37**, 43–48 (2016).
16. Pichon, M. et al. Where to biopsy to detect *Helicobacter pylori* and how many biopsies are needed to detect antibiotic resistance in a human stomach. *J Clin Med* **9**, 2812 (2020).
17. Shiotani, A., Roy, P., Lu, H. & Graham, D. Y. *Helicobacter pylori* diagnosis and therapy in the era of antimicrobial stewardship. *Therap. Adv. Gastroenterol* **14**, 17562848211064080 (2021).
18. Zarzecka, U. et al. Properties of the HtrA Protease From Bacterium *Helicobacter pylori* Whose Activity Is Indispensable for Growth Under Stress Conditions. *Front. Microbiol.* **10**, 961 (2019).
19. Zarzecka, U., Tegtmeier, N., Sticht, H. & Backert, S. Trimer stability of *Helicobacter pylori* HtrA is regulated by a natural mutation in the protease domain. *Med. Microbiol. Immunol.* **212**, 241–252 (2023).
20. Yamaoka, Y. & Graham, D. Y. *Helicobacter pylori* virulence and cancer pathogenesis. *Fut. Oncol.* **10**, 1487–1500 (2014).
21. Bénéjat, L. et al. Adaptation of an in-house PCR for the detection of *Helicobacter pylori* and the mutations associated with macrolide resistance into ready-to-use PCR microwell strips. *Helicobacter* **26**, e12855 (2021).
22. Souvorov, A., Agarwala, R. & Lipman, D. J. SKESA: strategic k-mer extension for scrupulous assemblies. *Genome Biol* **19**, 153 (2018).
23. Seemann, T. Prokka: rapid prokaryotic genome annotation. *Bioinformatics* **30**, 2068–2069 (2014).
24. Falush, D., Stephens, M. & Pritchard, J. K. Inference of population structure using multilocus genotype data: Linked loci and correlated allele frequencies. *Genetics* **164**, 1567–1587 (2003).
25. Falush, D. et al. Traces of human migrations in *Helicobacter pylori* populations. *Science* **299**, 1582–1585 (2003).

## Acknowledgements

The authors thank all the laboratories that sent gastric biopsies to our reference center, as well as the CRB-K of CHU Bordeaux for providing the paraffin blocks. This material constitutes original research and has not been previously published or submitted for publication elsewhere. We certify that Textcheck has reviewed and corrected the English in the manuscript. A specialist editor with appropriate professional qualifications (M.Sc., Ph.D., or M.D.) reviewed and corrected the English, and an English language specialist conducted a subsequent check. Both editors are native English speakers. Please direct any questions regarding the English in this certified paper to: [certified@textcheck.com](mailto:certified@textcheck.com) (reference number: 25052301).

## Author contributions

PL supervised the study. LG, CP, LB, MM, QJ, MR, GB, MP, PD, and PL analyzed the data and drafted the manuscript. CP and LB performed the experiments. All authors interpreted the data and critically revised the manuscript for important intellectual content.

## Funding

This work was supported by internal funding from the French National Reference Center for Campylobacters and Helicobacters provided by Santé Publique France, as well as by the Région Nouvelle-Aquitaine (PS-GAR-MIE project).

## Declarations

## Competing interests

The authors declare no competing interests.

## Human ethics and consent to participate declarations:

As the samples (human gastric DNA or the remaining FFPE samples) were sent to the NRCCH for research purpose only, therefore the need for ethical approval and informed consent has therefore not been waived by the ethics committee of the Bordeaux University hospital, as deemed unnecessary according to the scientific missions of the national reference center mandated by Santé Publique France ([www.spf.fr](http://www.spf.fr)) and published in the official journal of the French republic. All the *H. pylori* strains described in this study were anonymized and moved to the Centre de Ressources Biologiques from the Bordeaux University hospital (<https://www.chu-bor>

[deaux.fr/Professionnels-recherche/Centre-de-Ressources-Biologiques/](https://deaux.fr/Professionnels-recherche/Centre-de-Ressources-Biologiques/)). A Material Transfer Agreement was signed between the CRB and the National Reference Center for Campylobacters and Helicobacters (NRCCH) ([www.cnrch.fr](http://www.cnrch.fr)).

### Additional information

**Supplementary Information** The online version contains supplementary material available at <https://doi.org/10.1038/s41598-025-23540-8>.

**Correspondence** and requests for materials should be addressed to P.L.

**Reprints and permissions information** is available at [www.nature.com/reprints](http://www.nature.com/reprints).

**Publisher's note** Springer Nature remains neutral with regard to jurisdictional claims in published maps and institutional affiliations.

**Open Access** This article is licensed under a Creative Commons Attribution-NonCommercial-NoDerivatives 4.0 International License, which permits any non-commercial use, sharing, distribution and reproduction in any medium or format, as long as you give appropriate credit to the original author(s) and the source, provide a link to the Creative Commons licence, and indicate if you modified the licensed material. You do not have permission under this licence to share adapted material derived from this article or parts of it. The images or other third party material in this article are included in the article's Creative Commons licence, unless indicated otherwise in a credit line to the material. If material is not included in the article's Creative Commons licence and your intended use is not permitted by statutory regulation or exceeds the permitted use, you will need to obtain permission directly from the copyright holder. To view a copy of this licence, visit <http://creativecommons.org/licenses/by-nc-nd/4.0/>.

© The Author(s) 2025